Reversible Oligonucleosome Self-Association: Dependence on Divalent Cations and Core Histone Tail Domains†

Patricia M. Schwarz, Alicia Felthauser, Terace M. Fletcher, and Jeffrey C. Hansen*

Department of Biochemistry, The University of Texas Health Science Center at San Antonio, 7703 Floyd Curl Drive, San Antonio, Texas 78284-7760

Received October 27, 1995; Revised Manuscript Received February 6, 1996⊗

ABSTRACT: Regularly spaced nucleosomal arrays equilibrate between unfolded and highly folded conformations in <2 mM $MgCl_2$, and self-associate above 2 mM $MgCl_2$ [Schwarz, P. M., & Hansen, J. C. (1994) *J. Biol. Chem. 269*, 16284−16289]. Here we use analytical and differential sedimentation techniques to characterize the molecular mechanism and determinants of oligonucleosome self-association. Divalent cations induce self-association of intact nucleosomal arrays by binding to oligonucleosomal DNA and neutralizing its negative charge. Neither linker histones nor H2A/H2B dimers are required for Mg^{2+}-dependent self-association. However, divalent cations are unable to induce self-association of trypsinized nucleosomal arrays lacking their N- and C-terminal core histone tail domains. This suggests that the H3/H4 tail domains directly mediate oligonucleosome self-association through a non-Coulombic-based mechanism. Self-association occurs independently of whether the oligonucleosome monomers are folded or unfolded. The first step in the self-association pathway is strongly cooperative and produces a soluble association intermediate that sediments ∼10 times faster than the oligonucleosome monomers. The size of the oligonucleosome polymers increases rapidly as a consequence of small increases in the divalent cation concentration, eventually producing polymeric species that sediment at ≫10 000 S. Importantly, all steps in the self-association pathway are freely reversible upon removal of the divalent cations. Taken together, these data indicate that short oligonucleosome fragments composed of only core histone octamers and DNA possess all of the structural features required to achieve chromosome-level DNA compaction. These findings provide a molecular basis for explaining many of the recently uncovered structural features of interphase and metaphase chromosomal fibers.

Eukaryotic chromosomes are formed from hierarchical packaging of a long contiguous nucleosomal array. Largely due to the enormous complexity involved, the mechanisms that lead to formation of interphase and metaphase chromosomes are poorly understood. Most molecular studies have focused on the folding of extended 10 nm diameter nucleosomal arrays into compact 30 nm fibers, which is thought to be the initial step in the sequence of events that lead to chromosome formation. However, molecular analysis of even this simplest level of fiber organization has proven frustrating; after two decades of research there is still no general agreement as to either the structure or mechanism of formation of 30 nm chromatin fibers [reviewed in van Holde and Zlatanova, (1995), Woodcock and Horowitz (1995) and Wolffe (1995)]. Morphological studies of the higher order fiber organization of isolated chromosomes have produced equally equivocal conclusions. On one hand, metaphase chromosomes have been proposed to consist of both matrix-anchored radial loops and helical coils (Rattner & Lin, 1985; Boy de la Tour & Laemmeli, 1988). Alternatively, Belmont and Bruce (1994) have recently proposed that 30 nm chromatin fibers are successively folded into distinct 60−80 and 100−130 nm "chromonema" fibers, which are further folded and kinked to produce the 200−400 nm fibers characteristic of G1 chromatids. The ability to differentiate between various models is further complicated by the fact that extensive intermolecular fiber−fiber contacts obscure the visualization of discrete chromosomal fibers in the intact nuclei of most organisms (Giannasca et al., 1993). Despite the present uncertainties, all models of chromosome organization share one distinctive molecular characteristic. Packaging of a chromosomal DNA molecule into higher order chromosomal domains in some way involves long range interactions between chromatin segments that are widely separated on the contiguous chromosomal fiber.

Surprisingly few macromolecules have been shown to be involved in the formation and stabilization of eukaryotic chromosomes. Both topoisomerase II (Earnshaw et al., 1985) and the XCAP family of proteins (Hirano & Mitchison, 1994) are involved in the terminal condensation of metaphase chromosomes. However, there is no evidence that these proteins have important functions in organizing the higher order domains that make up the bulk of interphase chromosomal fibers. Surprisingly, one protein that clearly is *not* required for formation and maintenance of chromosomes is histone H1 (Ohsumi et al., 1993; Bouvet et al., 1994; Dasso et al., 1994; Shen et al., 1995). Consequently, at this point one must conclude that packaging of nucleosomal arrays into higher order chromosomal fibers either is entirely controlled by non-histone chromosomal proteins or is in part mediated by unidentified properties of the core histones.

For the purposes of identifying the contributions of the core histones to nuclear processes involving chromatin, we have been studying the solution-state behavior of defined oligonucleosome model systems reconstituted from core

† Supported by NIH Grant GM45916.

* To whom correspondence should be addressed: Tel: (210) 567-6980. FAX: (210) 567-6595. E-mail: hansen@bioc02.uthscsa.edu.

⊗ Abstract published in *Advance ACS Abstracts,* March 15, 1996.

0006-2960/96/0435-4009$12.00/0

histones and tandemly repeated 5S rDNA (Simpson et al., 1985). The ability to manipulate the composition and configuration of these model systems is unprecedented, as is the degree of structural homogeneity achieved after reconstitution. During the course of recent studies of Mg^{2+}-dependent oligonucleosome folding, it was observed that the 5S nucleosomal arrays self-associate at fractionally higher salt concentrations than are required to form folded 30 nm structures (Schwarz & Hansen, 1994). Salt-dependent self-association is a well documented property of native H1-containing chromatin fragments (Borochov et al., 1984; Ausio et al., 1986; Jin & Cole, 1986; Sen & Crothers, 1986; Widom, 1986; Rocha et al., 1986; Guo & Cole, 1989a,b). Several investigators have hypothesized that in vitro self-association is relevant to chromosome formation in vivo (Sen & Crothers, 1986; Widom, 1986). Alternatively, in vitro self-association may simply reflect irreversible formation of insoluble aggregates and have no biological relevance. This issue remains unresolved largely because of the nearly complete absence of mechanistic information about the self-association process.

To address this question, we have utilized 5S oligonucleosome model systems to characterize the molecular mechanism and macromolecular determinants of oligonucleosome self-association. Our results strongly support the interpretation that the mechanisms that govern in vitro self-association also participate in the stabilization of higher order chromosomal fibers in vivo. In addition, they suggest that a primary structural role of the core histone tail domains is to independently mediate both short range and long range compaction phenomena within eukaryotic chromosomes.

MATERIALS AND METHODS

Materials. Core histone octamers and H3/H4 tetramers were isolated from chicken erythrocytes as described previously (Hansen et al., 1989; Hansen & Wolffe, 1994). Trypsinized histone octamers lacking their amino- and carboxyl-terminal tail domains were prepared using the immobilized trypsin method of Ausio et al. (1989), as described in Fletcher and Hansen (1995). The 208-12 DNA template, which consists of 12 tandem 208 bp[1] repeats of *Lytechinus* 5S rDNA, was purified by digesting plasmid pPOL208-12 (Georgel et al., 1992) with 0.02 units of *HhaI* (Promega) per microgram of DNA for 96 h at 37 °C followed by Bio-Gel A150m exclusion chromatography (Hansen & Rickett, 1989). All chemicals were of reagent grade.

Oligonucleosome Reconstitution. Saturated and subsaturated 5S oligonucleosomes were reconstituted from intact chicken erythrocyte core histone octamers and 208-12 DNA by salt dialysis as described in Hansen and Lohr (1993). The mol of histone octamer/mol 208 of bp DNA (r) ranged from 0.4−1.2. The DNA concentration was 100 μg/mL. The final dialysis step was against 10 mM Tris-HCl, 0.25 mM EDTA, 2.5 mM NaCl, pH 7.8 (TEN) buffer. Immediately after reconstitution, oligonucleosomes were analyzed by sedimentation velocity in TEN buffer to determine the average number of histone octamers bound per DNA molecule (N) as described in Hansen and Lohr (1993). Saturation of the 5S repeats (i.e., $N = 12$) routinely was achieved at $r = 1.2$. Trypsinized histone octamer arrays and H3/H4 tetramer arrays were reconstituted by the same method outlined above. In these cases, template saturation was verified by comparing the average sedimentation coefficient measured in TEN buffer against that established previously for saturated trypsinized octamer arrays (Garcia-Ramirez et al., 1992; Fletcher & Hansen, 1995) and saturated H3/H4 tetramer arrays (Hansen et al., 1991). All reconstitutes were stored at 0−4 °C in the presence of 0.1 mM PMSF, 10 μg of aprotinin/mL, and 10 μg of leupeptin/mL.

Differential Centrifugation Assay for Oligonucleosome Self-Association. Formation of oligonucleosome homopolymers was ascertained using the intermolecular association assay described previously (Schwarz & Hansen, 1994). Briefly, reconstitutes were first diluted to $A_{260} \cong 1.6$ with TEN buffer. Reconstitutes and stock salt solutions (30 μL each) were mixed, incubated at room temperature for ≥5 min, and centrifuged in a Eppendorf microcentrifuge at 13 500 rpm (16 000g) for 10 min. The absorbance of the supernatant was then determined at 260 nm in a Hitachi U2000 double-beam spectrophotometer equipped with a 50 μL cell holder. Data were expressed as the percent of the sample that remained in the supernatant after centrifugation, (A_{260} of supernatant/original A_{260} in TEN) × 100.

Analytical Ultracentrifugation. Sedimentation velocity studies were carried out in a Beckman XL-A analytical ultracentrifuge equipped with scanner optics as described by Schwarz and Hansen (1994). Samples were equilibrated at the desired temperature for ≥30 min prior to the beginning of sedimentation. The oligonucleosome A_{260} ranged from 0.6 to 1.0. Sedimentation was at 4 000−28 000 rpm. The integral distribution of sedimentation coefficients was determined by analyzing 10−20 scans by the method of van Holde and Weischet (1978). In some cases, individual scans were analyzed according to the method of Goldberg (1958) to obtain the second moment sedimentation coefficient. Both types of analyses were performed using the Ultrascan data analysis software package (B. Demeler, Department of Biochemistry, University of Texas, Health Science Center at San Antonio).

RESULTS

Dependence of Oligonucleosome Self-Association on $MgCl_2$ Concentration and the Extent of Occupancy of 5S rDNA Repeats by Histone Octamers. The influence of $MgCl_2$ concentration on the self-association of saturated and subsaturated 208-12 oligonucleosomes is shown in Figure 1. In these experiments, formation of extensively associated oligonucleosome homopolymers was indicated by a decrease in the A_{260} of the supernatant after centrifugation in the microfuge (Schwarz & Hansen, 1994). Control experiments indicated that formation of pelletable oligonucleosome species was complete within one minute after exposure to salt (data not shown). Consistent with previous results, none of the samples showed evidence of self-association in <2 mM $MgCl_2$, (Schwarz & Hansen, 1994). However, all oligonucleosome samples formed large homopolymers in >2 mM $MgCl_2$. Both the maximum extent of self-association and the $MgCl_2$ concentration at which self-association was half maximal were strongly dependent on the extent of histone octamer saturation of the 208-12 DNA template. By contrast, naked 208-12 DNA remained unassociated in 0−500 mM $MgCl_2$ (data not shown).

[1] Abbreviations: bp, base pairs; N, number of nucleosomes bound per 208-12 DNA; EDTA, ethylenediaminetetraacetate, disodium salt; Tris-HCl, tris(hydroxymethyl)aminomethane hydrochloride; TEN, 10 mM Tris-HCl (pH 7.8), 0.25 mM Na_2EDTA, 2.5 mM NaCl; $s_{20,w}$, sedimentation coefficient at 20 °C in water.

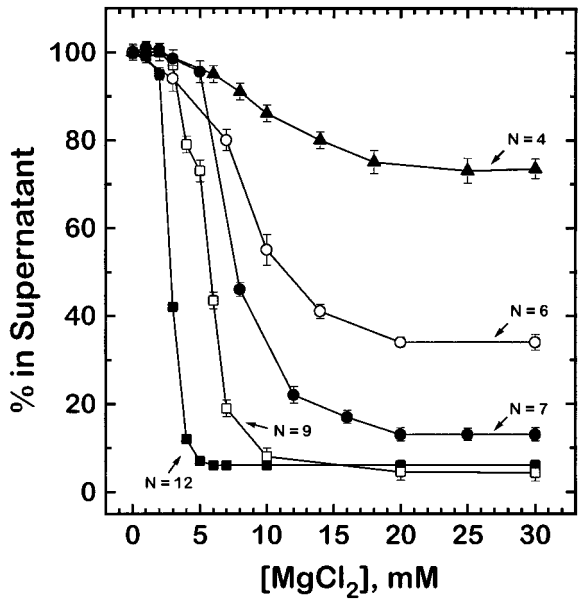

FIGURE 1: Self-association of both saturated and subsaturated oligonucleosome in $MgCl_2$. The effect of $MgCl_2$ on the extent of self-association of 208-12 oligonucleosomes containing an average (N) of 4 (▲), 6 (○), 7 (●), 9 (□), and 12 (■) nucleosomes/DNA template was determined using the differential centrifugation assay described under Experimental Procedures. Each data point represents the mean ± the standard deviation of three determinations.

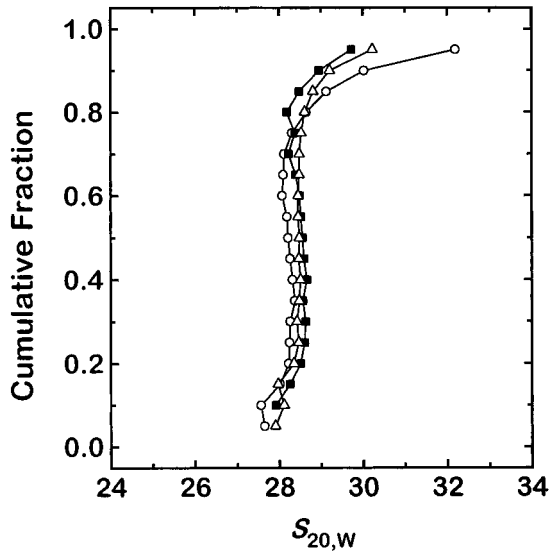

FIGURE 2: Reversibility of Mg^{2+}-dependent oligonucleosome self-association. Equal volumes of saturated 208-12 oligonucleosomes (N = 12) and $MgCl_2$ stock solutions were mixed to a final concentration of either 10 or 30 mM $MgCl_2$. The total volume of the samples was 530 μL. The A_{260} of a control sample prepared with TEN rather than $MgCl_2$ stocks was 0.78. The oligonucleosome polymers formed in $MgCl_2$ were pelleted by centrifugation for 10 min at 16 000g in the microfuge. The $MgCl_2$ supernatants were carefully removed and replaced with an equivalent volume (530 μL) of TEN buffer. Pellets were resuspended with gentle vortexing, transferred to dialysis membranes, dialyzed against TEN buffer for 12 h at 4 °C, and recentrifuged in the microfuge for 10 min at 16 000g. The A_{260} of the 10 and 30 mM $MgCl_2$ pellets after resuspension in TEN and recentrifugation were 0.77 and 0.78, respectively. Each of these supernatants was then subjected to sedimentation velocity in the analytical ultracentrifuge, and boundaries analyzed according to the method of van Holde and Weischet (1978). Shown are the sedimentation coefficient distributions obtained for the original oligonucleosome sample in TEN buffer (△), the 10 mM $MgCl_2$ pellet after resuspension in TEN buffer (■), and the 30 mM $MgCl_2$ pellet after resuspension in TEN buffer (○).

Mg^{2+}-Dependent Oligonucleosome Self-Association is Freely Reversible. The biological relevance of oligonucleosome self-association rests largely on its reversibility, yet this question has never been thoroughly investigated. We therefore performed the following experiment to determine whether Mg^{2+}-dependent self-association is reversible. Saturated 208-12 oligonucleosomes (N = 12) were first exposed to either 10 or 30 mM $MgCl_2$ to induce self-association of the entire sample. Oligonucleosome polymers formed under these conditions were then pelleted in the microfuge, $MgCl_2$ supernatants were removed, and the pellets were resuspended in an equivalent volume of TEN buffer. After dialysis against TEN buffer to remove residual traces of $MgCl_2$, samples were recentrifuged in the microfuge to pellet any remaining large oligonucleosome polymers, and the supernatants were collected. In both cases the A_{260} of these supernatants equaled that of the original sample in TEN buffer (see Figure 2 legend), indicating that the oligonucleosome polymers formed in 10 and 30 mM $MgCl_2$ quantitatively dissociated upon return to low salt conditions. The supernatants were also analyzed by sedimentation velocity in the analytical ultracentrifuge (Figure 2). The sedimentation coefficient distributions of the TEN-resuspended pellets and the original oligonucleosome sample also were identical, indicating that the oligonucleosome polymers formed in 10 and 30 mM $MgCl_2$ reverted to unfolded 29S oligonucleosome monomers in low salt buffer (Figure 2). Together, these results demonstrate unequivocally that Mg^{2+}-dependent oligonucleosome self-association is freely reversible.

Dependence of Oligonucleosome Self-Association on Cation and Anion Type. The relative effectiveness of different cations and anions at promoting oligonucleosome self-association is shown in Figure 3. To reproducibly achieve conditions where ~50% of the oligonucleosomes were self-associated in $MgCl_2$, these experiments were performed with subsaturated N = 7 nucleosomal arrays at divalent cation concentrations of 7 mM. Results indicated that the extent of self-association was strongly dependent on the divalent cation type; only 5% of the oligonucleosomes associated in $CdCl_2$, compared to 50% in $MgCl_2$ and >90% in $MnCl_2$. The relative effectiveness of divalent cations followed the relationship $Mn^{2+} \cong Zn^{2+} \gg Ba^{2+} > Mg^{2+} > Co^{2+} \gg Cd^{2+}$. No association was observed in the monovalent salts NaCl and CsCl at concentrations up to 600 mM (Figure 3; data not shown). The anion dependence generally was less pronounced than the cation dependence and followed the relationship acetate > Cl^- > Br^- = NO_3^- ≫ SO_4^{-2}. No association of the naked DNA template was observed in any of these salts at room temperature.

To ascertain the mechanism by which divalent cations induce oligonucleosome self-association, we measured the extent of self-association in mixtures of divalent and monovalent cations (Figure 4). In both 5 and 10 mM $MgCl_2$, increasing concentrations of KCl led to dramatic decreases in the fraction of the oligonucleosome sample that was associated. This result indicates that self-association is driven in part by divalent cation−DNA interactions (Widom, 1986; Clark & Kimura, 1990). It should be noted that in vitro transcription analyses of chromatin templates are generally performed in buffers containing both 5−10 mM free $MgCl_2$ and 50−100 mM KCl (Izban & Luse, 1991; Hansen & Wolffe, 1992). The data in Figure 4 indicate that functional assays performed under these ionic conditions may be susceptible to the influence of self-association.

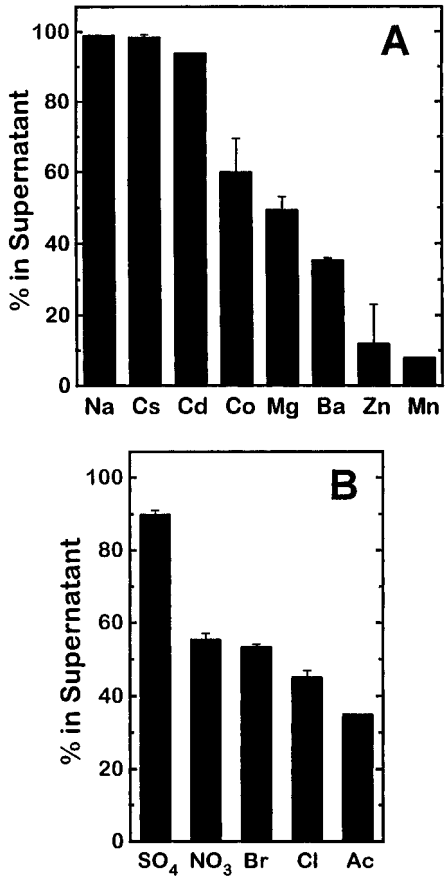

FIGURE 3: Cation and anion dependence of oligonucleosome self-association. (A) 208-12 oligonucleosomes ($N = 7$) were incubated in the chloride salts of the indicated cations for 5 min at 25 °C. In each case, the cation concentration was 7 mM. The extent of self-association was determined in triplicate using the differential centrifugation assay as described under Experimental Procedures. (B) $N = 7$ arrays were incubated in the Mg^{2+} salts of the indicated anions for 5 min at 25 °C. In each case, the Mg^{2+} concentration was 7 mM. The extent of self-association was determined in triplicate using the differential centrifugation assay as described under Experimental Procedures.

Mg^{2+}-Dependent Oligonucleosome Self-Association Requires Core Histone Tail Domains but Not H2A/H2B Dimers. The data in Figures 1 and 3 indicate that both divalent cations *and* core histone octamers contribute to the self-association mechanism. To further define the core histone determinants, we characterized the Mg^{2+}-dependent self-association of H3/H4 tetramer arrays and trypsinized nucleosomal arrays (Figure 5). Neither of these two types of "subnucleosomal" arrays is capable of Mg^{2+}-dependent folding (Hansen & Wolffe, 1994; Fletcher & Hansen, 1995). Somewhat surprisingly, saturated H3/H4 tetramer arrays exhibited virtually identical self-association behavior as intact nucleosomal arrays. By contrast, trypsinized nucleosomal arrays lacking their flexible tail domains did not self-associate to an appreciable extent. These data indicate that histone tail domains specifically mediate oligonucleosome self-association. In addition, they demonstrate that self-association occurs independently of whether the individual arrays are folded or unfolded.

Sedimentation Velocity Analysis of the Self-Association Mechanism. The studies described above have documented the reversibility of oligonucleosome self-association, and identified its molecular and macromolecular determinants. We next performed low-speed sedimentation velocity experiments to determine the distribution of species present at

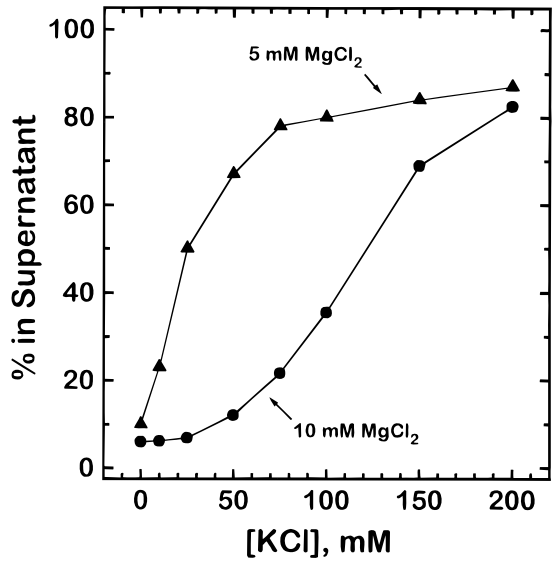

FIGURE 4: Effect of monovalent cations on Mg^{2+}-dependent oligonucleosome self-association. Saturated 208-12 oligonucleosomes were incubated in TEN buffer containing either 5 mM (▲) or 10 mM (●) $MgCl_2$ and the indicated concentrations of KCl. The extent of self-association was determined using the differential centrifugation assay described under Experimental Procedures. Each data point represents the average of two determinations.

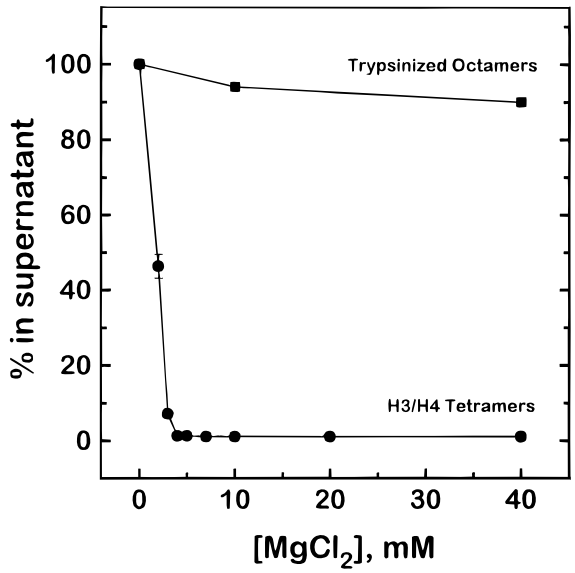

FIGURE 5: Effect of H2A/H2B dimer depletion and proteolytic removal of the core histone tail domains on Mg^{2+}-dependent self-association. The effect of $MgCl_2$ on the extent of self-association of saturated 208-12 trypsinized histone octamer arrays (■) and H3/H4 tetramer arrays (●) was determined using the differential centrifugation assay described under Experimental Procedures. Each data point represents the mean ± the standard deviation of three determinations.

intermediate extents of association. Under these conditions, a cooperative association mechanism would produce only monomers and extensively associated polymers. At the other extreme, an isodesmic association mechanism would produce all possible oligomeric species between the monomer and the most extensively associated polymer present under these conditions (i.e., monomers, dimers, trimers, ..., *n*-mers). In a sedimentation velocity experiment performed at rotor speeds that cause oligonucleosome monomers to sediment slowly, a cooperative mechanism would be indicated by the presence of two discrete boundaries, whereas an isodesmic

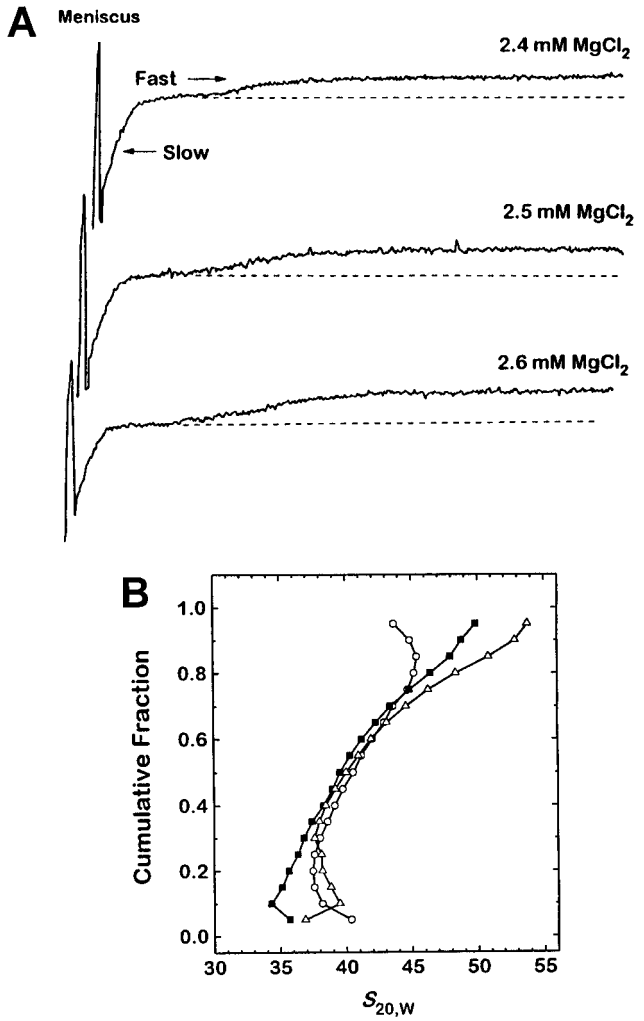

FIGURE 6: Sedimentation velocity analysis of the mechanism of formation of oligonucleosome homopolymers. Saturated 208-12 oligonucleosome were incubated in 2.4, 2.5, or 2.6 mM $MgCl_2$ and then sedimented in the analytical ultracentrifuge at either 4 000 or 16 000 rpm as described under Experimental Procedures. (A) Shown for each salt concentration is the scan obtained after ~75 min of sedimentation at 4 000 rpm. "Slow" and "fast" refer to the relative rates of movement of the two distinct boundaries present in these samples at this rotor speed. The dashed line indicates the nonsedimenting region that corresponds to the plateau of the slow boundary and the base line of the fast boundary. (B) Analysis of the slow boundaries by the method of van Holde and Weischet (1978). After collection of 12 scans at 4 000 rpm, the samples shown in panel A were recentrifuged at 16 000 rpm. At these higher speeds, only the portion of sample corresponding to the slow boundary of panel A was present, i.e., the material in the fast boundary pelleted prior to data collection. Shown are the sedimentation coefficient distributions obtained in 2.4 mM (△), 2.5 mM (■), and 2.6 mM (○) $MgCl_2$.

scheme would produce an amorphous region of faster sedimenting material at the top of the boundaries.

Representative low-speed sedimentation velocity scans of saturated 208-12 oligonucleosomes in 2.4, 2.5, and 2.6 mM $MgCl_2$ are shown in Figure 6A. Under these conditions, 22%, 26%, and 31% of the samples pelleted in the microfuge assay, respectively. At all three salt concentrations, the scans consisted of two distinct boundaries separated by a region of unchanging absorbance (indicated by the dashed lines). Furthermore, the fraction of the sample in the fast-moving boundaries was equivalent to that which pelleted in the microfuge assay. The integral distribution of sedimentation coefficients derived from the slow boundaries are shown in Figure 6B. These distributions are essentially identical to those observed previously for unassociated 208-12 oligonucleosome monomers in 1−2 mM $MgCl_2$ (Schwarz & Hansen, 1994). The sedimentation coefficient heterogeneity seen in Figure 6B reflects the fact that oligonucleosome monomers in the presence of Mg^{2+} equilibrate between the unfolded 29S state (see Figure 2) and an extensively folded ~55S species. The extent of compaction of the 55S species is equivalent to that of a classical 30 nm diameter "higher order" structure (see Schwarz & Hansen, 1994).

The fast-moving boundaries present in 2.4−2.6 mM $MgCl_2$ showed considerable spreading during sedimentation, suggesting that they were composed of a moderately heterogeneous population of oligonucleosome polymers. Because the total absorbance of the fast boundaries was too small to allow accurate determination of the $s_{20,w}$ distribution, these boundaries were analyzed by the second moment method. The second moment point in a sedimentation velocity boundary effectively yields a weight average sedimentation coefficient (Goldberg, 1958). When plotted against the scan number, the second moment $s_{20,w}$ derived from eight successive boundaries decreased systematically in all three salt concentrations (data not shown). Such a decrease would be expected if the fastest sedimenting components of a heterogeneous sample pelleted during the time interval between successive scans. Extrapolation of these plots to zero time yielded a second moment $s_{20,w}$ of ~500 S, ~650 S, and ~800 S for the associated oligonucleosome species present in 2.4, 2.5, and 2.6 mM $MgCl_2$, respectively (data not shown).

In summary, the data in Figure 6 yield three important conclusions regarding the self-association mechanism. First, only oligonucleosome monomers and extensively associated oligonucleosome polymers were present under ionic conditions that produced intermediate extents of association. Second, the size distribution of oligonucleosome polymers present under these conditions was moderately heterogeneous. Finally, very small increases in $MgCl_2$ concentration simultaneously led to decreased amounts of oligonucleosome monomers and large increases in the average size of the oligonucleosome polymers.

We next determined whether a highly subsaturated oligonucleosome preparation containing an average of five histone octamers per 208-12 DNA molecule ($N = 5$) exhibited the same association behavior as that identified in Figure 6 for saturated oligonucleosomes. At a $MgCl_2$ concentration that led to pelleting of ~10%−15% of the total sample in the differential centrifugation assay (i.e., 25%−35% of the maximum extent of association observed for these subsaturated samples), sedimentation velocity scans were composed of two distinct boundaries separated by a region of unchanging absorbance (data not shown). Analysis of the scans by the second moment (Table 1) and integral distribution (not shown) methods indicated that the slow sedimenting boundaries consisted entirely of *unfolded* 16S oligonucleosome monomers. The inability of highly subsaturated 208-12 oligonucleosomes to undergo Mg^{2+}-dependent folding has been observed previously (Fletcher et al., 1994). Nonetheless, the average second moment $s_{20,w}$ derived from the fast moving boundaries was ≥10 times larger than that of the oligonucleosome monomers and increased with increasing extents of association (Table 1). Thus, both saturated and highly subsaturated oligonucleosomes exhibit the same general association behavior, despite the fact that the subsaturated arrays are unfolded.

Table 1: Sedimentation Velocity Analysis of the Self-Association of Highly Subsaturated 208-12 Oligonucleosomes

$MgCl_2$ (mM)	%[a]	s_{slow}[b]	s_{fast}[c]
0	0	15.2	
8	10	16.3	174
10	14	16.7	294

[a] These values indicate the percent of an $N = 5$ oligonucleosome sample that pelleted in the microfuge assay at the indicated $MgCl_2$ concentrations. The maximum extent of self-association of this sample observed in 30 mM $MgCl_2$ was 51%. [b] These values refer to the average second moment $s_{20,w}$ derived from 12−14 successive scans collected at rotor speeds of 24 000 rpm. [c] These values represent the average second moment $s_{20,w}$ derived from four to six fast-moving boundaries (such as those in Figure 6A) collected at rotor speeds of 4 000 rpm.

DISCUSSION

Molecular Mechanism and Structural Determinants. Oligonucleosome self-association is strongly dependent on divalent cation type, relatively weakly dependent on anion type, and does not occur in monovalent salts. The ability of monovalent salts to reduce the extent of self-association at any given divalent cation concentration indicates that the association process is driven by divalent cation binding to oligonucleosomal DNA (Widom, 1986; Clark & Kimura, 1990). Even extensively associated oligonucleosome polymers that sediment at ≫10 000S (see below) dissociate into unfolded monomers upon removal of salt, indicating that all steps in the association pathway are freely reversible (Figure 2). Furthermore, both association and dissociation are rapid, reaching equilibrium within 1 min after exposure to high salt or low salt conditions, respectively (data not shown). In addition to divalent cations, oligonucleosome self-association is critically dependent on specific properties provided by the core histones as indicated by the following findings: (1) naked DNA does not self-associate under the ionic conditions of our experiments, (2) both the maximum extent of association and the salt concentration at which self-association is 50% maximal are affected by the degree of histone octamer saturation of the DNA template (Figure 1), and (3) proteolytic removal of the core histone "tail" domains inhibits Mg^{2+}-dependent self-association (Figure 5). From these observations we conclude that reversible oligonucleosome self-association is mediated both by the degree of DNA charge neutralization, and by separate function(s) provided by core histone tail domains. Interestingly, although core histone tail domains also specifically mediate salt-dependent oligonucleosome folding (Garcia-Ramirez et al., 1992, 1995; Fletcher & Hansen, 1995), self-association occurs independently of whether the oligonucleosomes are folded or unfolded (Figure 5, Table 1). Considering that only the H3/H4 tail domains appear to be required for self-association (Figure 5), these observations together suggest that folding and self-association may be mediated by different actions and (or) subsets of the tail domains. Although more work will be required to resolve these questions, the supranucleosomal functions provided by the core histone tail domains clearly are more diverse and mechanistically complex than previously has been appreciated.

Two distinct types of association behavior are involved in the formation of oligonucleosome homopolymers. Under salt conditions that induce association of only a small fraction of the total oligonucleosome sample, we detect only unassociated monomers and a population of *soluble* polymers that sediment ≥10 times faster than the unassociated monomers; intermediate sized species such as dimers or trimers are never observed (Figure 6, Table 1). These data indicate that the initial step in the association pathway is highly cooperative. At higher $MgCl_2$ concentrations, we continue to detect only monomeric and extensively associated oligonucleosome species. However, salt-dependent decreases in the amount of oligonucleosome monomers are coupled to increases in the average size of the oligonucleosome polymers (Figure 6; Table 1). Eventually, ionic conditions that induce association of the entire oligonucleosome sample produce polymeric species that pellet in the analytical ultracentrifuge within 3 min at 3 000 rpm, and hence must sediment at ≫10 000 S (data not shown). Taken together, these results indicate that extensively associated oligonucleosome polymers are formed through the combination of an initial cooperative step and a second step that is isodesmic in nature.

Implications for Interphase and Metaphase Chromosome Structure. The studies described above demonstrate that short linear nucleosomal arrays composed of only core histone octamers and DNA possess an almost infinite capacity to cooperatively and reversibly self-associate given sufficient neutralization of DNA charge. Two situations can be envisioned in which the intrinsic self-association properties of nucleosomal arrays are likely to contribute to the structure of intact chromosomes. The first case involves the intermolecular interactions that occur between segments of different chromosomes. Giannasca et al. (1993) have recently suggested that such interfiber interactions occur extensively in most organisms, often to the point where they obscure organized fiber structure within individual chromosomes (McDowall et al., 1986; Giannasca et al., 1993).

The second situation involves long-range intrafiber interactions. Interphase chromosomal fibers behave as intrinsically flexible polymers in situ (van den Engh et al., 1992; Sachs et al., 1995). Hence, the same properties that lead to Mg^{2+}-dependent self-association of short oligonucleosome fragments in vitro should also promote interactions between widely separated regions of a chromosome-length nucleosomal array in vivo. Cell biological studies have provided experimental evidence in support of such a relationship. For example, highly condensed heterochromatin is present within intact nuclei *only* if the nuclei are isolated in the presence of ≥2 mM Mg^{2+}; under lower salt conditions the heterochromatin decondenses (Olins & Olins, 1972; Aaronson & Woo, 1981; Weith, 1982; Langmore & Paulson, 1983; Dixon & Burkholder, 1985). This indicates that the fiber−fiber interactions that stabilize heterochromatin are strongly Mg^{2+}-dependent. Further evidence is provided by the recent work of Belmont and Bruce (1994), who characterized changes in interphase chromosome structure during progression through G1 stage of the cell cycle. In addition to 10−30 nm chromatin filaments and 200−400 nm G1 chromatids, these investigators visualized two intermediate levels of chromosomal fiber structure. These intermediate "chromonema" fibers were 60−80 and 100−130 nm in diameter and exhibited a twisted, supercoiled morphology. Consistent with both the properties of oligonucleosome self-association in vitro and the earlier studies of heterochromatin stability in intact nuclei, chromonema fiber stability was found to be critically dependent on multivalent cation concentration, i.e., when chromosomes were isolated in buffers containing low levels of Mg^{2+} or polyamines, organization above the 30 nm fiber was not observed (Belmont et al., 1989; Belmont

& Bruce, 1994). In addition, although a hierarchical relationship was found to exist between 10−30 nm chromatin filaments, chromonema fibers, and G1 chromatids (Belmont et al., 1989; Belmont & Bruce, 1994), the apparent coexistence of both unfolded 10 nm filaments and folded 30 nm chromatin fibers within 60−80 nm chromonema fibers (Belmont & Bruce, 1994) suggests that local chromatin folding is mechanistically uncoupled from formation of higher order chromonema domains. Mg^{2+}-dependent oligonucleosome folding and self-association also are hierarchically related, but mechanistically distinct (Figures 1, 4, and 6; Table 1; Schwarz & Hansen, 1994). The uncoupling of short-range and long-range DNA compaction mechanisms also helps explain the findings that chromosome condensation and decondensation involves simultaneous changes at several different organizational levels rather than a sequential folding/unfolding process (Belmont et al., 1989; Belmont & Bruce, 1994). Finally, chromonema fiber condensation/decondensation was found to be reversible and appeared to involve cooperative interactions over large DNA lengths (Belmont et al., 1989; Belmont & Bruce, 1994).

The numerous key molecular characteristics shared by in vitro oligonucleosome self-association and the in situ packaging of chromosomal fibers support the interpretation that oligonucleosome self-association is an in vitro manifestation of the long-range intra- and interfiber interactions involved in stabilizing interphase and metaphase chromosomes. An important prediction stemming from our interpretation is that chromosome-level DNA compaction can be achieved in nuclei in the complete absence of linker histones. Precisely this result has been obtained recently for both isolated nuclei (Dasso et al., 1994) and metaphase chromosomes (Ohsumi et al., 1993) and in the nuclei of living cells (Bouvet et al., 1994; Shen et al., 1995). Finally, while we have proposed that intrinsic functions provided by the core histone tail domains of nucleosomal arrays contribute much of the driving force for *bulk* chromosome condensation and heterochromatin formation, the specific structure of any given stretch of a chromosomal fiber almost certainly will also be shaped by its specific complement of non-histone chromosomal proteins, e.g., HP1, polycomb, and SIR3 [see Eissenberg (1989) and Wolffe (1995) for reviews].

ACKNOWLEDGMENT

We thank Isabelle Kreider and Cynthia Turgeon for excellent technical assistance.

REFERENCES

Aaronson, R. P., & Woo, E. (1981) *J. Cell Biol. 90*, 181−186.
Ausio, J., Sasi, R., & Fasman, G. D. (1986) *Biochemistry 25*, 1387−1403.
Ausio, J., Dong, F., & van Holde, K. E. (1989) *J. Mol. Biol. 206*, 451−463.
Belmont, A. S., & Bruce K. (1994) *J. Cell Biol. 127*, 287−302.
Belmont, A. S., Braunfeld, M. B., Sedat, J. W., & Agard, D. A. (1989) *Chromosoma 98*, 129−143.
Borochov, Ausio, J., & Eisenberg, H. (1984) *Nucleic Acids Res. 12*, 3089−3096.
Bouvet, P., Dimitrov, S., & Wolffe, A. P. (1994) *Genes Dev. 8*, 1147−1159.
Boy de la Tour, E., & Laemmli, U. K. (1988) *Cell 55*, 937−944.
Clark, D. J., & Kimura, T. (1990) *J. Mol. Biol. 211*, 883−896.
Dasso, M., Dimitrov, S., & Wolffe, A. P. (1994) *Proc. Natl. Acad. Sci. U.S.A. 91*, 12477−12481.
Dixon, D. K., & Burkholder, G. D. (1985) *Eur. J. Cell Biol. 36*, 315−322.
Earnshaw, W. C., Halligan, B., Cooke, C. A., Heck, M. M. S., & Liu, L. F. (1985) *J. Cell Biol. 100*, 1706−1715.
Eissenberg, J. C. (1989) *BioEssays 11*, 14−17.
Fletcher, T. M., & Hansen, J. C. (1995) *J. Biol. Chem. 270*, 25359−25362.
Fletcher, T. M., Serwer, P., & Hansen, J. C. (1994) *Biochemistry 33*, 10859−10863.
Garcia-Ramirez, M., Dong, F., & Ausio, J. (1992) *J. Biol. Chem. 267*, 19587−19595.
Garcia-Ramirez, M., Rocchini, C., & Ausio, J. (1995) *J. Biol. Chem. 270*, 17923−17928.
Georgel, P., Demeler, B., Terpening, C., Paule, M. R., & van Holde, K. E. (1993) *J. Biol. Chem. 268*, 1947−1954.
Giannasca, P. J., Horowitz, R. A., & Woodcock, C. L. (1993) *J. Cell Sci. 105*, 551−561.
Goldberg, R. J. (1958) *J. Phys. Chem. 57*, 194−202.
Guo X. W., & Cole, R. D. (1989a) *J. Biol Chem. 264*, 16873−16879.
Guo X. W., & Cole, R. D. (1989b) *J. Biol. Chem. 264*, 11653−11657.
Hansen, J. C., & Rickett, H. (1989) *Anal. Biochem. 179*, 167−170.
Hansen, J. C., & Wolffe, A. P. (1992) *Biochemistry 31*, 7977−7988.
Hansen, J. C., & Lohr, D. (1993) *J. Biol. Chem. 268*, 5840−5848.
Hansen, J. C., & Wolffe, A. P. (1994) *Proc. Natl. Acad. Sci. U.S.A. 91*, 2339−2343.
Hansen, J. C., Ausio, J., Stanik, V. H., & van Holde, K. E. (1989) *Biochemistry 28*, 9129−9136.
Hansen, J. C., van Holde, K. E., & Lohr, D. (1991) *J. Biol. Chem. 266*, 4276−4282.
Hansen, J. C., Lebowitz, J., & Demeler, B. (1994) *Biochemistry 33*, 13155−13163.
Hirano, T., & Michison, T. J. (1994). *Cell 79*, 449−458.
Izban, M. G., & Luse, D. S. (1991) *Genes Dev. 5*, 683−696.
Jin, Y., & Cole, R. D. (1986) *J. Biol. Chem. 261*, 15805−15812.
Langmore, J. P., & Paulson, J. R. (1983) *J. Cell Biol. 96*, 1120−1131.
McDowall, A. W., Smith, J. M., & Dubochet, J. (1986) *EMBO J. 5*, 1395−1402.
Ohsumi, K., Katagiri, C., & Kishimoto, T. (1993) *Science 262*, 2033−2035.
Olins, D. E., & Olins, A. (1972) *J. Cell Biol. 53*, 715−736.
Rattner, J. B., & Lin, C. C. (1985) *Cell 42*, 291−296.
Rocha, E., Davie, J. R., van Holde, K. E., & Weintraub, H. (1984) *J. Biol. Chem. 259*, 8558−8563.
Sachs, R. K., van den Engh, G., Trask, B., Yokota, H., & Hearst, J. E. (1995) *Proc. Natl. Acad. Sci. U.S.A. 92*, 2710−2714.
Schwarz, P. M., & Hansen, J. C. (1994) *J. Biol. Chem. 269*, 16284−16289.
Sen, D., & Crothers, D. (1986) *Biochemistry 25*, 1495−1503.
Shen, X., Yu, L., Weir, J. W., & Gorovsky, M. A. (1995) *Cell 82*, 47−56.
Simpson, R. T., Thoma, F., & Brubaker, J. M. (1985) *Cell 42*, 799−808.
van den Engh, G., Sachs, R., & Trask, B. J. (1992) *Science 257*, 1410−1412.
van Holde, K. E., & Weischet, W. O. (1978) *Biopolymers 25*, 1981−1988.
van Holde, K. E., & Zlatanova, J. (1995) *J. Biol. Chem. 270*, 8373−8376.
Weith, A. (1983) *Exp. Cell Res. 146*, 199−203.
Widom, J. (1986) *J. Mol. Biol. 190*, 411−424.
Wolffe, A. P. (1995) *Chromatin: Structure and Function*, 2nd ed., Academic Press, New York.
Woodcock, C. H., & Horowitz, R. (1995) *Trends Cell Biol. 5*, 272−277.

BI9525684